Photoluminescence Properties of Eu(TTA)$_3$Phen/PS-PMMA Polymer Blend Electrospun Nanofibers

Manjusha Dandekar[1,a], Sangeeta Itankar[1,b], S. B. Kondawar[2,c]

[1] *Department of Physics, G.H. Raisoni Skill Tech University, Nagpur - 440033, India.*
[1] *Department of Physics, Suryodaya College of Engineering and Technology, Nagpur 440016, India*
[2] *Department of Physics, Rashtrasant Tukadoji Maharaj Nagpur University, Nagpur - 440033, India*

[a] manjusha.dandekar@gmail.com
[b] skawadkar18@gmail.com
[c] sbkondawar@yahoo.co.in

Abstract

Because of their 4f electrons, europium metal ions have incredibly crisp emission bands. As the overlaying 5s^2 and 5p^6 orbitals effectively protect 4f orbitals from the effects of external pressures. Complex forms of europium metal ions, such Eu(TTA)$_3$Phen, have garnered a lot of concentration for of their high fluorescence emission efficiency, which is caused by the ligands' high absorption coefficient. The Europium complex Eu(TTA)$_3$Phen doped PS-PMMA polymer mix, Eu (TTA)$_3$Phen/PS, and Eu (TTA)$_3$Phen/PMMA have been synthesized and reported here. The SEM picture, XRD and PL characterizations, and CIE chromaticity were used to characterize the synthesized nanofibers made using the electrospinning technology. The f–f electron transition of Eu^{3+} ions and the antenna effect of ligands provide this Europium β-diketon complex exceptional optical and luminous characteristics. Due to the extreme hypersensitive behaviour of the $^5D_0 \rightarrow {}^7F_2$ transition, the photoluminescence emission spectrum of nanofibers exhibits very high intense red emission. Because Eu3+ ions separate in the polymer chain of molecules, there will be more contact between the polymer and Europium complexes, which explains why polymers, polystyrene (PS), and polymethyl methacrylate (PMMA) have good optical properties. This was made possible by the polymer nanofibers' even distribution of Eu^{3+}. This is because the presence of polymer may cause the site symmetry of the Eu^{3+} ion to decrease, and the surrounding polymer media may distort it. This study demonstrates the possible use of electrospinning in a variety of polymer optoelectronic devices and emphasises its promising uses in the creation of protective textiles. Because electrospun nanofibers are strong, flexible, and have exceptional photoluminescence qualities, they are used in the newest technology for smart textiles to create smart fabrics for a variety of applications. These textiles provide as protection against a wide range of environmental threats.

Keywords: E-Textile Electrospinning method, Europium nanofibers, Photoluminescence.
Received 31 January 2025; First Review 19 February 2025; Accepted 21 February 2025.

*** Address of correspondence**
Manjusha Dandekar
Department of Physics, G.H. Raisoni Skill Tech University, Nagpur - 440033, India

Email: manjusha.dandekar@gmail.com

How to cite this article
Manjusha Dandekar, Sangeeta Itankar, S. B. Kondawar, Photoluminescence Properties of Eu(TTA)$_3$Phen/PS-PMMA Polymer Blend Electrospun Nanofibers, J. Cond. Matt. 2025; 03 (01): 71-77.

Available from:
https://doi.org/10.61343/jcm.v3i01.131

Introduction

Due to their distinctive luminescence characteristics, including extremely crisp emission bands, a long lifespan, and the possibility for high internal quantum competence, photoactive rare-earth Eu complexes in particular, europium β-diketones are of both technical and essential interest [1]. These Eu β-diketon complexes have remarkable optical and luminous properties due to the f–f electron transition of Eu^{3+} ions and the antenna effect of ligands, which opens up important possibilities [2–4]. However, the pure Eu complexes have limited practical applications and only show promise for comprehensive photophysical applications due to their poor comprehensive photophysical applications due to their poor mechanical strength, poor thermal stability, low processing ability, and poor resistance to air moisture.

Europium complexes are typically added to organic or inorganic hybrid matrices, sol–gel silica [6], or organically modified silicates and polymers, to create powders, fibres, thin solid films, etc., as a suitable way to get around these drawbacks. Eu complex-doped polymers have garnered a lot of attention due to their mechanical flexibility and ability to retain the complexes' luminescent characteristics while being processed from solution. It has been a steady increase in interest in polymer materials. There are now several ways to produce thin polymer films. Technically and financially,

polymeric materials constitute the most significant class of organic materials [7].

The polymers added RE complexes are mechanically flexible and have enhanced photoluminescence and thermal stability [8-9]. Rare earth complexes added to polymeric systems are anticipated to be used in functional devices such tiny lasers, waveguide amplifiers, and polymer fibre lasers, which are a significant component of the rapidly expanding area of photonics [10-12].

Electrospinning is a reasonably simple and efficient approach for creating fibres with a variety of compositions, long lengths, and uniform diameters when compared to other production methods [13]. With this method, a polymer solution droplet's surface is charged with a high voltage, which causes a liquid jet to be ejected via a spinneret [14]. The jet is then repeatedly stretched to create continuous, ultrafine fibres as a result of bending instability. Fibres made with this technique can have widths ranging from a few nanometres to several micrometres [15]. Nanofibers produced by the electrospinning process have several notable characteristics, such as pore sizes in the nano range, a very high surface area to volume ratio, unique physical characteristics, and the ability to be functionalised and modified chemically and physically [16–17].

Method

The optimum technique for creating Eu(TTA)$_3$Phen/Polymer nanofibers is electrospinning. Electrospinning is a somewhat simple and efficient approach for creating fibers with a variety of compositions, long lengths, and uniform diameters when compared to other fabrication methods. Fibers made with this technique can have sizes ranging from a few nanometers to several micrometers.

The solution approach was employed to create the europium complex Eu(TTA)$_3$Phen used in this investigation [1]. Figure 1 below illustrates the chemical mechanism via which Eu(TTA)$_3$Phen is created.

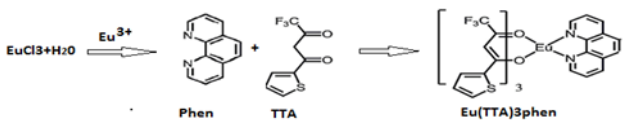

Figure 1: Chemical process of formation of Eu(TTA)$_3$Phen

Synthesis method of Eu(TTA)$_3$Phen/PMMA Composite Solutions

Following the creation of the Eu(TTA)$_3$Phen complex, several polymers, including PS (mol. wt = 350,000) and PMMA (mol. wt = 350,000), used to create Eu(TTA)$_3$Phen/Polymer composite solutions. A standard procedure for making Eu(TTA)$_3$Phen/PS involved dissolving 2g of PS in 10ml of THF (tetrahydrofuran) solvent and stirring it magnetically for 12 hours until it was homogenous. The aforesaid uniform PS polymeric solution was then magnetically agitated for 12 hours until uniform, after which 20% of Eu(TTA)$_3$Phen complex powder was added. For synthesis of Eu(TTA)$_3$Phen/PMMA and Eu(TTA)$_3$Phen/PMMA-PS polymer blend, same procedure was carried out again.

Discussion

SEM Image of Prepared Electrospun Nanofibers

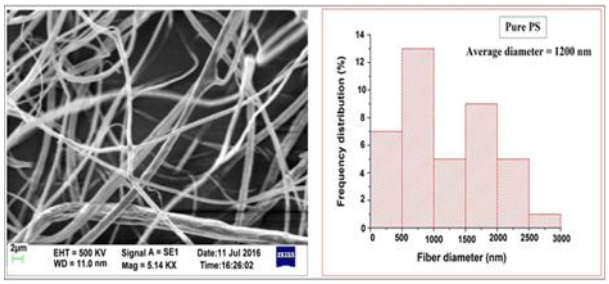

Figure 2: SEM image with histogram of PS nanofibers.

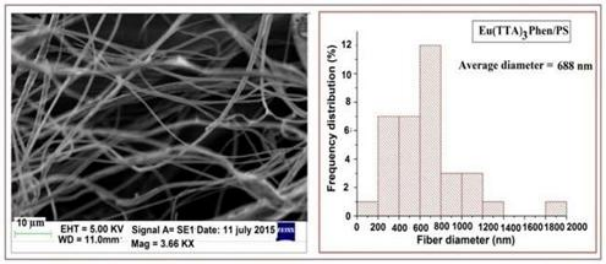

Figure 3: SEM image with histogram of Eu(TTA)$_3$Phen/PS nanofibers.

Figures 2 and 3 display the SEM image with histogram of pure Polystyrene and Eu(TTA)$_3$Phen/PS composite electrospun nanofibers, separately. Because bending instability brought on by the spinning jet and stationary collector, it exhibits morphologically nanofibrous characteristics, with a uniform diameter and variable orientation alignment. It is clear from comparing the fibre morphologies of pure Polystyrene and Eu(TTA)$_3$Phen/PS that the composite nanofibers have lower average diameters (about 688 nm) than pure Polystyrene. This might be the result of the electrospinning solution's improved conductivity brought on by the addition of Eu(TTA)$_3$Phen. Based on the Polystyrene nanofibers histogram analysis, the average fibre diameter was determined to be between 1200 and 1200 nm. However, for Eu(TTA)$_3$Phen/PS, it was 688 nm, demonstrating that the morphology of the electrospinning fibres may be effectively improved by adding the europium complex to the polymer matrix.

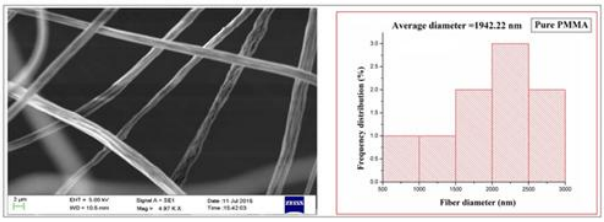

Figure 4: SEM image with histogram of PMMA nanofibers.

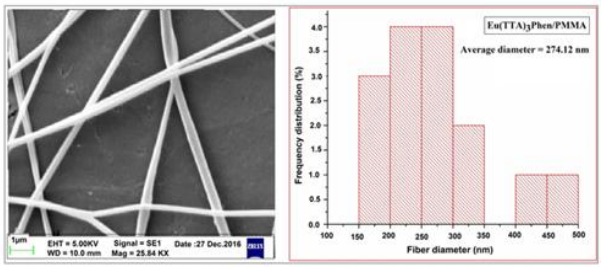

Figure 5: SEM image with histogram of Eu(TTA)$_3$Phen/PMMA nanofibers.

Figures 4 and 5 display the morphologies of uniform nanofibers of PMMA and Eu(TTA)$_3$Phen/PMMA that were generated with diameter ranging from 500 to 2000 nm. Due to the bending instability brought on by the spinning jet, all of the nanofibers have the same diameter, are aligned, and are orientated randomly. The typical diameter of the fibres was determined to be 1942.22 nm for pure PMMA and 274.12 nm for Eu(TTA)$_3$Phen/PMMA based on the analysis of the nanofiber histogram. The composite nanofibers average diameters are clearly smaller than those of the pure PMMA. This demonstrates the same cause of the electrospinning solution's improved conductivity brought on by the addition of PMMA to Eu(TTA)$_3$Phen.

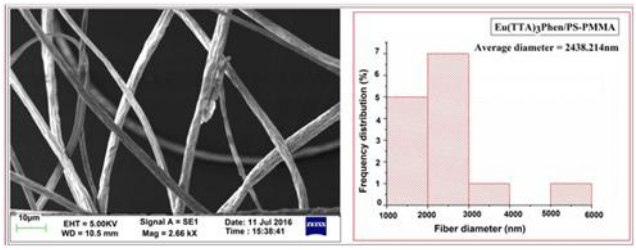

Figure 6: SEM image with histogram of Eu(TTA)$_3$Phen/PS-PMMA nanofibers.

The morphologies of the electrospun Eu(TTA)$_3$Phen/PS-PMMA composite nanofibers are displayed in Figure 6, which indicates that the bending instability linked to the spinning jet caused the nanofibers to align in a random orientation and have a uniform diameter. The nanofibers were discovered to be arbitrarily orientated on the collector because of the fixed collector and the twisting variability carried on by the electrospinning jet [16]. Based on the analysis of nanofiber historiography, the average fiber diameter was determined to be between 2438.21 nm.

XRD of Eu(TTA)$_3$Phen/PS Polymer Composite Nanofibers

Figure 7 displays the XRD result of pure PS, Eu(TTA)$_3$Phen complex, and Eu(TTA)$_3$Phen/PS composite. The range of XRD result points is 2θ = 10 to 60 degrees. The diffraction peak for pure PS nanofibers in the X-ray diffraction was at about 15.21 with plane (300), indicating that the sample was primarily amorphous. Another peak, representing the monoclinic structure of the PS unit cell, appears at 16.80 with plane (220) and 18.250 with plane (211).

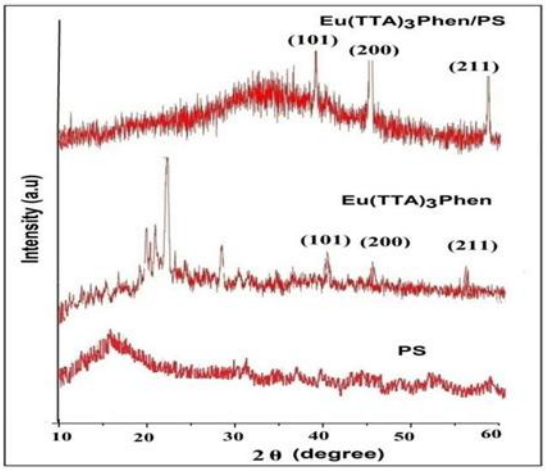

Figure 7: XRD pattern of Eu(TTA)$_3$Phen/PS.

The XRD result of the Eu(TTA)$_3$Phen complex showed well-resolved peaks at 20.26, 21.64, 21.66, 27.80. These peaks confirmed the crystalline behaviour of Eu(TTA)$_3$Phen. These strongest diffractive peaks make it abundantly evident that the Eu(TTA)$_3$Phen combination is a particular type of crystal [29]. Eu(TTA)$_3$Phen/PS X-ray diffraction almost displays a large peak of europium, indicating the presence of chemical interaction between the polymer PS and the Europium complex. PS matrices have been found to dominate the crystallinity of Eu(TTA)$_3$Phen upon the addition of polymers. It is apparent, sharp peaks of the Eu(TTA)$_3$Phen/PS have disappeared.

XRD of Eu(TTA)$_3$Phen/PMMA Fibres

Figure 8 displays the XRD result of pure PMMA, Eu(TTA)$_3$Phen, and Eu(TTA)$_3$Phen/PMMA composite. PMMA nanofibers XRD patterns display three distinctive peaks at 2θ = 29.5°, 42.5°, and 52.5°, which correspond to planes (111), (220), and (311). The non-crystalline character of pure PMMA is confirmed by the absence of any strong diffraction peaks. However, when a polymer is added to Eu(TTA)$_3$Phen/PMMA, the crystallinity of Eu(TTA)3phen is dominated by Polymer matrices. It is apparent that the distinct diffraction peaks of the Eu(TTA)$_3$Phen/PMMA pure complex have vanished. When mixing with PMMA, certain additional features appear; the

peak locations differ somewhat from pure complex. This suggests that the matrix PMMA has an impact on the complex's crystal structure, possibly as a result of the coordination with PMMA distorting the local environment of Eu^{3+} [31].

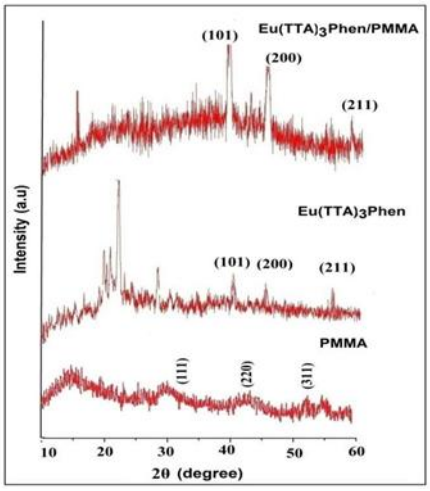

Figure 8: XRD pattern of $Eu(TTA)_3Phen$/PMMA.

Figure 9 displays the $Eu(TTA)_3Phen$/PS-PMMA composite's XRD result. It shows that the tiny matching peaks of europium have been found in the range of $2\theta = 15°$ to 58°. This finding suggests that in polymer blend matrices presence of $Eu(TTA)_3Phen$ [34].

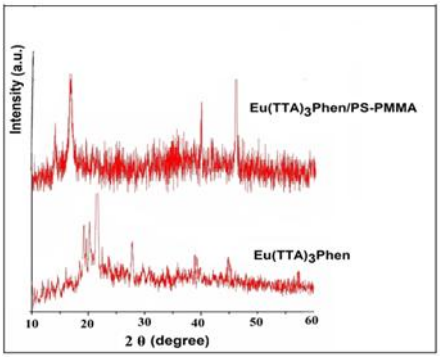

Figure 9: XRD pattern of $Eu(TTA)_3Phen$/PS-PMMA composite.

Photoluminescence in $Eu(TTA)_3Phen$

Figure 10 shows the excitation spectra of the pure $Eu(TTA)_3$phen compound at 354 nm. The ligands $\pi \rightarrow \pi^*$ electron transport results in a broad excitation band that extends from 255 to 455 nm [27–31]. Every excitation band shows blue shift and splits into two components, with peaks at roughly 271 and 346 nm, respectively.

The site symmetry of the Eu^{3+} ion may be reduced and deformed by the surrounding polymer media in the composite nanofibers. The $^7F_0 \rightarrow ^5D_2$ and $^7F_1 \rightarrow ^5D_1$ excitation lines are visible in the excitation spectrum of pure $Eu(TTA)_3Phen$, but they disappear in the composite fibres. This suggested that the f–f inner-shell transitions in the composite fibres would be quenched by the nonradiative energy transfer from the higher excited states to specific unknown defect levels, which took the place of the nonradiative relaxation from higher excited states to the $^5D_0$ level [28].

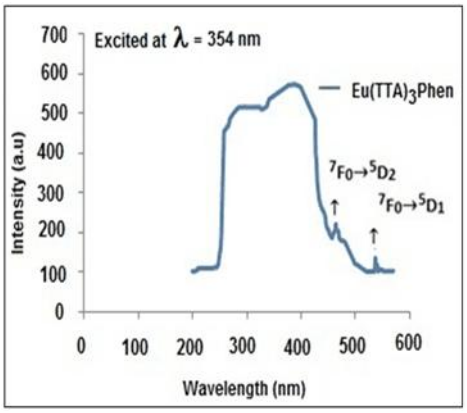

Figure 10: The excitation spectra of the $Eu(TTA)_3Phen$ complex.

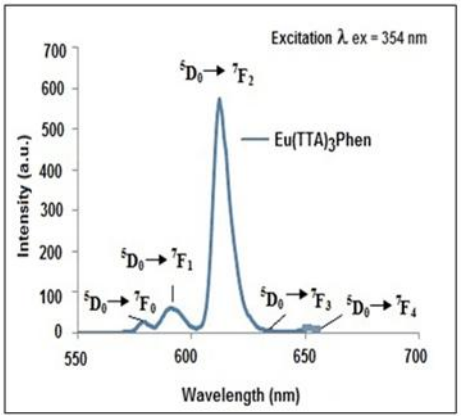

Figure 11: The emission spectra of the $Eu(TTA)_3Phen$ complex.

Figure 11 displays the $Eu(TTA)_3Phen$ complexes emission spectra. Under stimulation at 354 nm, the emission spectra of $Eu(TTA)_3Phen$ were measured between 550 and 655 nm [27–32]. The four emission peaks, at 579, 592, 612, 642, and 654 nm, are caused by the f–f transitions of Eu^{3+}. In that order, their designations are $^5D_0 \rightarrow ^7F_0$, $^5D_0 \rightarrow ^7F_1$, $^5D_0 \rightarrow ^7F_2$, $^5D_0 \rightarrow ^7F_3$, and $^5D_0 \rightarrow ^7F_4$. The Eu^{3+} ion is found in a single chemical environment when there is just one $^5D_0 \rightarrow ^7F_0$ line. The Eu^{3+} ion is in a single site without a centre of inversion, as evidenced by the $^5D_0 \rightarrow ^7F_2$ transitions far higher intensity than the other transitions. The $^5D_0 \rightarrow ^7F_1$ transition is a magnetic dipole transition among them.

The various excitation spectra of $Eu(TTA)_3Phen$/Polymers composites triggered at 354 nm are displayed in Figure 12. A wide excitation band spanning from 250 to 450 nm is produced by the ligands' $\pi \rightarrow \pi^*$ electron transfer in the case of the pure $Eu(TTA)_3Phen$ complex [33].

On the other hand, the excitation bands of Eu(TTA)$_3$Phen/Polymer composites exhibit blue shift and split in half, peaking at approximately 270 and 345 nm, respectively. This is because the presence of polymer may cause the site symmetry of the Eu^{3+} ion to be reduced and the surrounding polymer media to distort it.

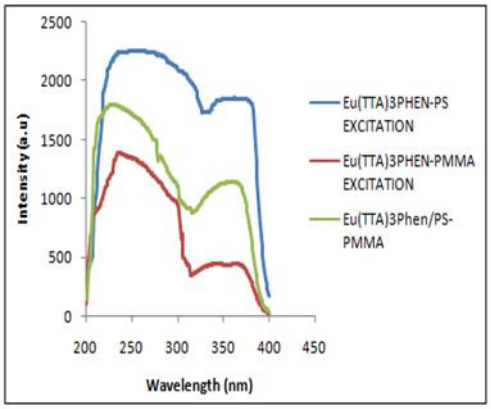

Figure 12: Excitation Spectra of Eu(TTA)$_3$Phen/Polymer composites nanofibers.

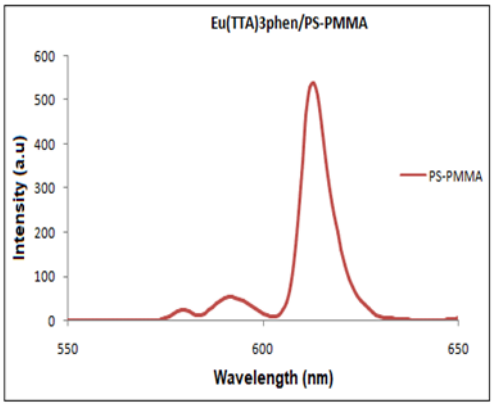

Figure 13: Emission Spectra of Eu(TTA)$_3$Phen/PS-PMMA composite nanofibers.

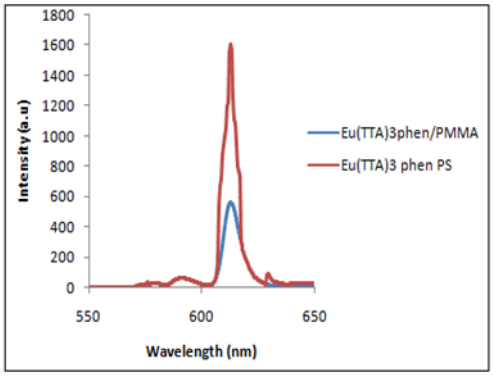

Figure 14: Emission Spectra of Eu(TTA)$_3$Phen/Polymers composite nanofibers.

Figure 13 and Figure 14 displays the Eu(TTA)$_3$Phen/Polymers composites emission spectra, which were obtained under excitation at 354 nm and ranged

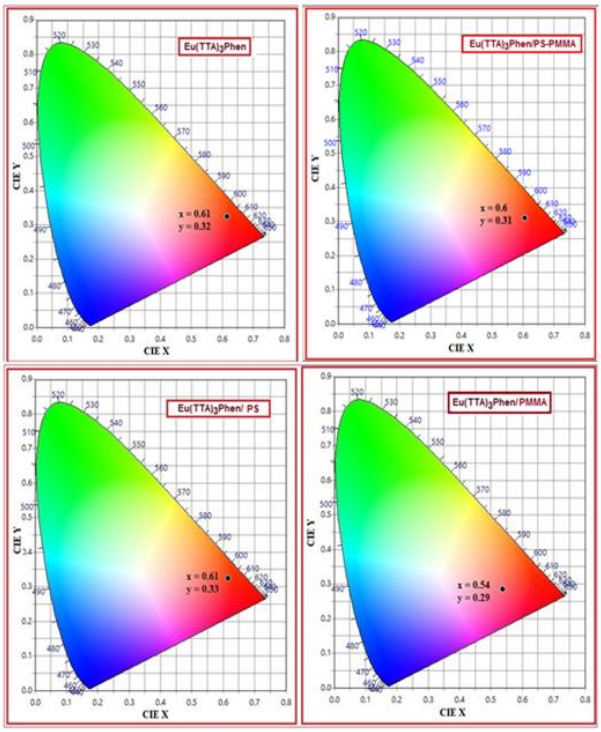

Figure 15: CIE chromaticity color coordinates for (a) Eu(TTA)$_3$Phen (b) Eu(TTA)$_3$Phen/PVDF.

from 550 to 655 nm. Four emission peaks are identified as being associated with the $^5D_0 \rightarrow {}^7F_0$, $^5D_0 \rightarrow {}^7F_1$, $^5D_0 \rightarrow {}^7F_2$, and $^5D_0 \rightarrow {}^7F_3$, respectively, and are centered at 579, 592, 612, and 652 nm. The usual red emission of the Eu^{3+} ion, attributed to the transitions between the multiplet ($^7F_{0-4}$) and the first excited state ($^5D_0$), made up the room-temperature fluorescence spectra of the composite nanofibers.

The presence of the Eu(TTA)$_3$Phen complex in polymers frequently results in a higher luminous intensity than the pure complex because the complex is equally distributed along the macromolecular chains of the polymers. Because Eu(TTA)$_3$Phen/Polymers fibers are electro spun nanofibers, their luminescent complex is distributed similarly to that of the macromolecular chain of polymers, and their luminous intensity is higher than that of bulk material [25].

Therefore, the results indicated above imply that the presence of polymers like PS and PMMA frequently increases the fluorescence intensity of the $^5D_0 \rightarrow {}^7F_2$ sensitivity transition of Eu^{3+} ions. When integrated into the microcavities of the polymer matrix, the europium complexes exhibit more disordered local surroundings due to the impact of the surrounding polymer [26]. The emission intensity increases as if the ions were excited at nearly the same wavelength when Eu^{3+} ions are implanted in a different polymer matrix.

CIE Chromaticity Coordinates

Using PL emission data, the CIE coordinates of the

$Eu(TTA)_3Phen$ complex, $Eu(TTA)_3Phen$/Polymers, and polymer blends were obtained using the Commission Internationale de l'Eclairage (CIE), Colour calculator software, shown in figure 15. The permissible CIE values for the red emission of the $Eu(TTA)_3Phen$ complex are x = 0.61 and y = 0.32 coordinates (Figure 13), which are close to the coordinates for pure red emission set by the National Television System Committee (NTSC) [14–16].

The CIE coordinates of the $Eu(TTA)_3Phen$ complex moved from their original location and showed good colour saturation upon the addition of a polymer. The calculated CIE coordinates are x = 0.61, y=0.33 for $Eu(TTA)_3Phen$/PS, x = 0.54, y = 0.29 for $Eu(TTA)_3Phen$/PMMA, and x = 0.6, y = 0.31 for $Eu(TTA)_3Phen$/Polymer-Polymer mix. The calculated CIE shows good colour saturation. As the europium complex doped polymers matrix was seen, the emission intensity increased and the CIE colour coordinates moved towards pure or saturated red emission. The complex's integrated polymer matrix emitted saturated red light, and its CIE colour coordinates were red.

Conclusion and Future Prospective

The synthesis, characterisation, and photoluminescence characteristics of $Eu(TTA)_3Phen$, $Eu(TTA)_3Phen$/Polymer composites, and $Eu(TTA)_3Phen$/Polymer-Polymer blends electrospun nanofibers made by electrospinning process are the main topics of the current study. Photoactive lanthanide complexes such as europium with β-diketones are highly interesting due to their high emission peaks in the visible and near-infrared region under UV stimulation. However, the rare-earth ions can enhance this by forming complexes with organic ligands.

The ligand $Eu(TTA)_3Phen$ may absorb far more light than the Eu^{3+} ions because the chromophores of the organic ligand have very strong absorption bands. These ligands can act as an antenna and fill the emitting excited levels by absorbing the excitation light and transferring the excitation energy to the higher energy levels of the Eu^{3+} ion. The fashion industry is becoming more interested in safety clothing as a result of the development of luminous textile materials. In addition to being beneficial in a variety of textile applications, the ability to generate light without heat without the need for an external power source is also appealing. In order to create clothing that can catch and emit light so that it is always visible, even in the dark, for a specified amount of time, the invention pertains to a photoluminescent fabric and a method of creating one.

References

1. Y. Hongquan, L. Tao, B. Chen, Y. Wua, Y. Li, *"Preparation of aligned $Eu(DBM)_3Phen$/PS fibers by electrospinning and their luminescence properties"*, Journal of Colloid and Interface Science, 2, (2013), 231-521.
2. Z. Xiaoping, W. Shipeng, H. Shui, Z. Liqun, L. Liu, *"Electrospinning preparation and luminescence properties of $Eu(TTA)_3Phen$ /polystyrene composite nanofibers"*, Journal of rare earths, 28, (2010), 332-337.
3. R. Hassey, J. Swain, N. Hammer, D. Venkataraman, M. Barnesm, *"Probing the chiroptical response of a single molecule"*, J. Science, 314, (2006), 1437-1452.
4. M. Robinson, J. Ostrowski, G. Bazan, M. Mcgehee, *"Reduced operating voltages in polymer light-emitting diodes Doped with rare-earth complexes"*, J. Adv. Mater., 15, (2003), 1547-1552.
5. M. Abdullah, T. Morimoto, K. Okuyama, *"Generating blue and red luminescence from zno/poly (ethylene glycol) nanocomposites prepared using an in-situ method"*, J. Adv. Funct. Mater, 13, (2003), 800-816.
6. B. Edison, G. Gibelli, J. Kai, E.S. Ercules, Teotonio, L. Oscar, C. Malta, *"Photoluminescent PMMA polymer films doped with Eu^{3+} diketonate crown ether complex"*, Journal of Photochemistry and Photobiology A: Chemistry, 251, (2013), 154–159.
7. K. Binnemans, Rare-earth beta-diketonates, in: K. A. Gschneidner Jr., J.-C. G. Bünzli, V. K. Pecharsky (Editors.), Handbook on the Physics and Chemistry of Rare Earths, Elsevier, Amsterdam, 35, (2004), 107–272.
8. J. C. G. Bünzli, *"Lanthanide luminescence for biomedical analyses and imaging"*, Chemical Reviews, 110, (2010), 2729–2755.
9. H. F. Brito, O. L. Malta, M. C. F. C. Felinto, E. E. S. Teotonio, *"Luminescence phenomena involving metal enolates, in: J. Zabicky (Ed.), Patai Series: The Chemistry of Metal Enolates"*, John Wiley & Sons Ltd, Chichester, England, 1, (2009), 131–184.
10. S. V. Eliseeva, J. C. G. Bünzli, *"Lanthanide luminescence for functional materials and bio-sciences"*, Chemical Society Reviews, 39, (2010), 189–227.
11. M. C. Felinto, C. S. Tomiyama, H. F. Brito, E.S. Teotonio, O. L. Malta, *"Synthesis and luminescent properties of supramolecules of b-diketonate of Eu(III) and crown ethers as ligands"*, Journal of Solid State Chemistry, 171, (2003), 189–194.
12. H. F. Brito, O.L. Malta, L. R. Souza, J. F. S. Menezes, C. A. Carvalho, *"Luminescence of the films of Europium(III) with thenoyltrifluoro acetonate and macrocyclic"*, Journal of Non-Crystalline Solids, 247, (1999), 129–133.

13. K. Sheng, B. Yan, *"Coordination bonding assembly and photophysical properties of Europium organic/inorganic/polymeric hybrid materials"*, Journal of Photochemistry and Photobiology A: Chemistry, 206, (2009), 140–147.
14. X. Ouyang, R. Yu, J. Jin, J. Li, R. Yang, W. Tan, J. Yuan, *"New strategy for label-free and time-resolved luminescent assay of protein: conjugate Eu^{3+} complex and aptamer-wrapped carbon nanotubes"*, J.Analytical Chemistry, 83, (2011), 782–789.
15. A. K. Singh, S. K. Singh, H. Mishra, R. Prakash, S. B. Rai, *"Structural, thermal, and fluorescence properties of $Eu(DBM)_3Phenx$ complex doped in PMMA"*, Journal of Physical Chemistry B, 114, (2010), 13042–13051.
16. P. Lenaerts, K. Driensen, R. V. Deun, K. Binnermans, *"Covalent coupling of luminescent tris (2-thenoyltrifluoroacetonato)lanthanide(III) complexes on a merrifield resin"*, J. Chemistry of Materials, 17, (2005), 2148–2154.
17. J. Kai, M. C. F. C. Felinto, L. A. O. Nunes, O. L. Malta, H. F. Brito, *"Intermolecular energy transfer and photostability of luminescence-tuneable multicolour PMMA films doped with lanthanide"*, J. Chemistry of Materials, 11, (2011), 125-132.
18. E. Drexler, *"Engines of Creation: The Coming Era of Nanotechnology"*, Publisher Doubleday, 1, (1986), 54-85.
19. *"Nanoscience and nanotechnologies: opportunities and uncertainties"*, J. Royal Society and Royal Academy of Engineering. Published by Clyvedon press, 2, (2004), 25.
20. C. Buzea, I. Pacheco, K. Robbie, *"Nanomaterials and Nanoparticles: Sources and Toxicity"*, J. Biophysical Chemistry Biointerphase, 2, (2007), 17-71.
21. H. Singh, P. Nalwa, *"Synthesis and processing"*, Handbook of Nanostructured Materials and Nanotechnology, 21, (2004), 424-632.
22. Nanotechnology information Center: Properties, Application, Resarch and safety Guideline, American Elements, 5, (2011), 63-74.
23. Allhoff, Fritz; Lin, Patrick, Moore, Daniel, *"what is nanotechnology and why does it matter? From science to ethics"*, P.John Wiley and Sons, 1, (2009), 304-336.
24. S. K. Prasad, *"Modern Concepts in Nanotechnology"*, Discovery Publishing House. 1, (2008), 31-32.
25. Kahn, Jennifer, *"Nanotechnology"*. National Geography, 12, (2006), 98–119.
26. P. Chouhan, Dr. R. Clarkson, *"Nanotechnology: changes and challenges for world"*, international journal of Innovative Research in Engineering & Science, 2, (2016), 13-53.
27. S. Mashaghi, T. Jadidi, G. Koenderink, A. Mashaghi, *"Lipid Nanotechnology"*, Int. J. Mol. Sci. 14, (2013), 4242-4282.
28. N. Kattamuri, J. H. Shin, B. Kang, C. G. Lee, J. K. Lee, C. Sung, *"Development and surface characterization of positively charged filters"*, J. Mater Sci., 40, (2005), 4531–4539.
29. W. Margaret, Frey, Lei Li, *"Electrospinning and Porosity Measurements of Nylon-6 / Poly(ethyleneoxide) Blended Nonwovens"*, Journal of Engineered Fibers and Fabrics, 2, (2007), 63-68.
30. Kenrya, Chwee Teck Limb, *"Nanofiber technology: current status and emerging developments"*, J. Progress in Polymer Science, 2, (2017), 124–165.
31. J. M. Deitzel, J. Kleinmeyer, D. Harris, *"The effect of processing variables on the morphology of electrospun nanofibers and textiles"*, J. Polymer, 42, (2001), 261– 72.
32. A. K. Haghi, M. Akbari, *"Trends in electrospinning of natural nanofibers"*, J. Phys Status Solid, 204, (2007), 1830–1844.
33. S. Sukigara, M. Gandhi, J. Ayutsede, M. Micklus, *"Regeneration of Bombyx mori silk by electrospinning Part2. Process optimization and empirical modeling using response surface methodology"*, J. Polymer 45, (2004), 3701–3708.
34. P. K. Baumgarten, *"Electrostatic spinning of acrylic microfibers"*, J Colloid Interface Sci, 36, (1971), 71–79.